Crystalline Films of Interdigitated Structures Formed via Amidinium−Carboxylate Interactions at the Air−Water Interface

Ivan Kuzmenko,[||] Maik Kindermann,[§] Kristian Kjaer,[†] Paul B. Howes,[†] Jens Als-Nielsen,[‡] Rony Granek,[||] Gunther v. Kiedrowski,*[,§] Leslie Leiserowitz,*[,||] and Meir Lahav*[,||]

Contribution from the Department of Materials and Interfaces, The Weizmann Institute of Science, 76100 Rehovot, Israel, Organic Chemistry 1, Ruhr-University Bochum, D-44780 Bochum, Germany, Materials Research Department, Risø National Laboratory, DK 4000, Roskilde, Denmark, and Niels Bohr Institute, H. C. Ørsted Laboratory, DK 2100, Copenhagen, Denmark

Received July 14, 2000

Abstract: Electrostatic interactions between amidinium and carboxylates were used for the construction of interdigitated architectures at the air−solution interface. Spreading the water-insoluble amphiphile *p*-pentadecylbenzoic acid (*A*) on an aqueous solution of *p*-methylbenzamidinium (*B*) ions results in an intercalation of the water-soluble base between the acidic headgroups of the water-insoluble amphiphile to form an amorphous *A-B-A-B* monolayer according to grazing incidence X-ray diffraction (GIXD) and X-ray reflectivity measurements. Upon compression the monolayer transforms into a crystalline film composed of three bilayers with interdigitated hydrocarbon chains, and a top layer whose chains are disordered. Water-insoluble *p*-heptadecylbenzamidinium spread on an aqueous solution of benzoic acid displays a surface pressure−area isotherm similar to that obtained from the above system. A mechanism that accounts for the formation of these films is presented. Deposition of *p*-heptadecylbenzamidinium and *p*-pentadecylbenzoic acid amphiphiles in a 1:1 ratio on pure water led to the formation of a crystalline monolayer phase but which is partially disordered. Over an aqueous solution containing a 1:1 mixture of benzamidinium and benzoic acid no measurable binding of these solute molecules to the polar headgroups of the 1:1 mixed monolayer could be detected by X-ray reflectivity or GIXD.

Introduction

Here we have focused on two aspects of the assembly of molecules into two-dimensional (2D) and 3D arrays. The first is linked to the design of interdigitated films. As already demonstrated, long-chain acid molecules (pentadecyl *R*-mandelic acid), when spread on aqueous solutions containing a water-soluble amine (*R*-phenylethylamine), form a 1:1 acid−base monolayer on the solution that is amorphous owing to the poor packing between the hydrocarbon chains. Upon compression, such a film transforms into a crystalline interdigitated bilayer and a top layer containing disordered hydrocarbon chains.[1] The process of interdigitation at the interface is remarkably sensitive to the molecular and chiral composition of the acid and base components, suggesting further elaboration. In the present study, we take advantage of electrostatic interactions between amidinium and carboxylic acid functions (Scheme 1) as the starting building blocks. These structures are of importance in biological systems containing arginine-active sites.[2−5] Simple chemical systems based on these interactions were extensively studied in aqueous and in nonaqueous solutions.[6−12] Strong hydrogen bonds of the type N−H···O−C between amidinium (or guani-

Scheme 1

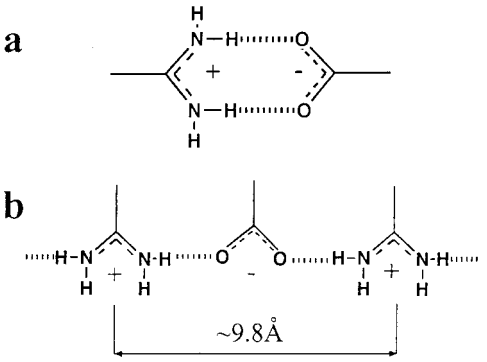

[||] The Weizmann Institute of Science.
[§] Ruhr-University Bochum.
[†] Risø National Laboratory.
[‡] Niels Bohr Institute.

(1) Kuzmenko, I.; Buller, R.; Bouwman, W. G.; Kjaer, K.; Als-Nielsen, J.; Lahav, M.; Leiserowitz, L. *Science* **1996**, *274*, 2046.
(2) Adams, J. M.; Buehner, M.; Chandrasekhar, K.; Ford, G. C.; Hackert, M. L.; Liljas, A.; Rossman, M. G.; Smiley, J. E.; Allison, W. S.; Everse, J.; Kaplan, N. O.; Taylor, S. S. *Proc. Natl. Acad. Sci. U.S.A.* **1973**, *70*, 1968.
(3) Eventoff, W.; Rossmann, M. G.; Taylor, S. S.; Torff, H. J.; Meyer, H.; Keil, W.; Kiltz, H. H. *Proc. Natl. Acad. Sci. U.S.A.* **1977**, *74*, 2677.
(4) Christianson, D. W.; Lipscomb, W. N. *Proc. Natl. Acad. Sci. U.S.A.* **1986**, *83*, 7568.
(5) Roderick, S. L.; Banszak, L. J. *J. Biol. Chem.* **1986**, *261*, 9461.
(6) Andres, J.; Moliner, V.; Krechl, J.; Silla, E. *J. Chem. Soc., Perkin Trans. 2* **1995**, 1551.
(7) Krechl, J.; Smrckova, S.; Pavlikova, F.; Kuthan, J. *Collect. Czech. Chem. Commun.* **1989**, *54*, 2415.
(8) Krechl, J.; Bohm, S.; Smrckova, S.; Kuthan, J. *Collect. Czech. Chem. Commun.* **1989**, *54*, 673.
(9) Krechl, J.; Bohm, S.; Smrckova, S.; Kuthan, J. *Collect. Czech. Chem. Commun.* **1989**, *54*, 673.
(10) Krechl, J.; Smrckova, S.; Kuthan, J. *Collect. Czech. Chem. Commun.* **1990**, *55*, 460.
(11) Krechl, J.; Smrckova, S.; Ludwig, M.; Kuthan, J. *Collect. Czech. Chem. Commun.* **1990**, *55*, 469.
(12) Krechl, J.; Smrckova, S. *Collect. Czech. Chem. Commun.* **1989**, *30*, 5315.

10.1021/ja002597o CCC: $20.00
Published on Web 03/29/2001

Scheme 2

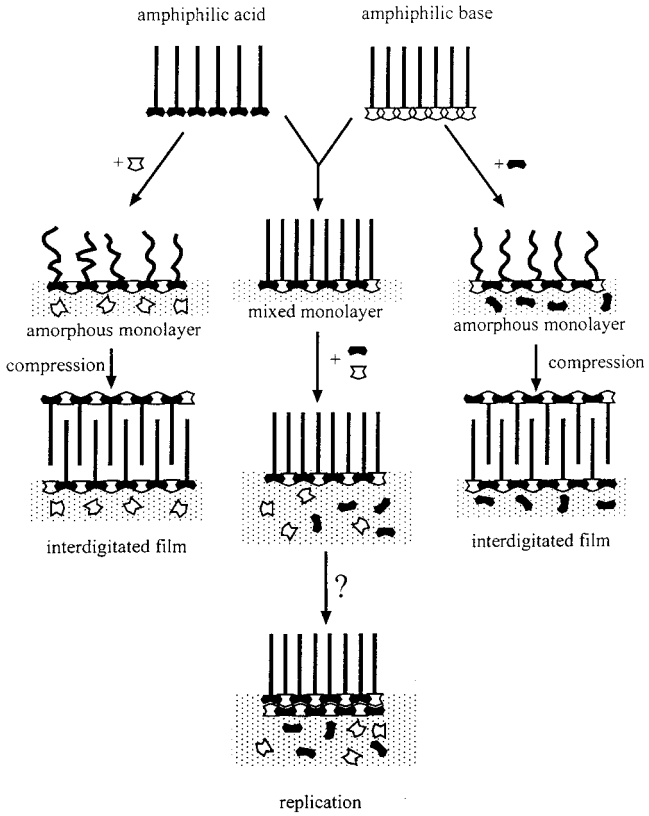

dinium) and carboxylic moieties existing in nonpolar solutions were employed for the design of supramolecular architectures[13,14] and in artificial self-replicating systems that mimic natural molecular self-replication and might shed light on the origin of evolution of living systems.[15,16] The strong electrostatic interactions between carboxylate and amidinium moieties would thus appear suitable to guarantee the formation of a mixed monolayer of the *-A-B-A-B-*type, where *A* is the amphiphilic acid moiety and *B* the water-soluble base (or vice versa). The hydrocarbon chains bound to the *A* headgroups in the extended *-A-B-A-B-*type rows are poorly packed so that such a monolayer should be amorphous but, upon compression, transform into a crystalline interdigitated multilayer (Scheme 2, right and left).

Our second goal was to examine the potential replicating properties of the system at the air−water interface as a result of binding of the water-soluble amidinium and carboxylic components to the polar headgroups of the preformed mixed monolayer containing the same chemical functions, as depicted in Scheme 2 (middle). The water-soluble amidinium and benzoic acid molecules in the subphase, if bound to the mixed monolayer interface in an ordered way, may be designed to react with each other to form a polymer system and thus initiate a self-replicating system in a manner akin to self-replicating systems in bulk solutions.[15]

2. Experimental Section

2.1. Synthesis. General Procedures. ^{1}H NMR spectra were recorded on a DPX-200 Bruker spectrometer (200 MHz) in $CDCl_3$ and DMSO-[d_6] using TMS as an internal standard. Multiplicities in ^{1}H NMR spectra are reported as broad (br), singlet (s), doublet (d), triplet (t), quartet (q), and multiplet (m). Thin-layer chromatography (TLC) was performed on Macherey-Nagel polygram silica plates, and column chromatography was performed on ICN silica gel 32−63.

Hexadecyltriphenylphosphoniumbromide, 1. To a suspension of triphenylphosphane (25.0 g, 95 mmol) in 180 mL of acetonitrile was added 1-bromohexadecane (29.0 g, 98 mmol). The mixture was refluxed overnight, the solvent removed in vacuo, and the resulting yellow oil treated several times with dry diethyl ether to yield a white precipitate (38.8 g, 80%).

4-(Heptadec-1-enyl)benzonitrile, 2. A solution of *n*-hexadecyltriphenylphosphoniumbromide (38.8 g, 68 mmol) in 120 mL of dry THF was treated with *n*-butyllithium (2.5 M in *n*-hexane, 28 mL, 70 mmol), resulting in a bright orange solution. The mixture was stirred for 1 h, and *p*-cyanobenzaldehyde (9.18 g, 70 mmol), dissolved in 50 mL of THF, was added dropwise over a period of 2 h. After stirring for 15 h at room temperature the reaction mixture was quenched with 12 mL of acetone, stirred for an additional hour, and filtered over a short column of neutral aluminum oxide to remove all triphenylphosphaneoxide. The solvent was evaporated and the solid residue recrystallized from methanol, yielding **2** (14.04 g 60%): mp 51 °C. ^{1}H NMR (250 MHz, $CDCl_3$): δ = 0.88 (t, J = 7.4 Hz, 3H, CH3), 1.17−1.39 (m, 24H, 12-H-24-H), 1.45 (q, J = 7.3 Hz, 2H, 11-H), 2.18−2.35 (m, Ar−CH═CH−CH_2), 5.81 (dt, J = 11.6 Hz, J = 7.5 Hz, 1H, Ar−CH═C$\underline{H}$), 6.35−6.43 (m, 1H, Ar−CH═C$\underline{H}$), 7.31−7.42 (m, 2H, 3-H, 5-H), 7.53−7.64 (m, 2H, 2-H, 6-H).

4-Heptadecylbezonitrile, 3. 4-(Heptadec-1-enyl)benzonitrile (8.0 g, 23.6 mmol) was hydrogenated overnight under normal pressure in 100 mL of a solvent mixture (ethyl acetate:methanol, 1:1) containing 200 mg of Pd/C (10%) as the hydrogenation catalyst under normal pressure. The catalyst was removed by filtration over Celite, and the solvent was evaporated. The residue was purified by chromatography on silica gel (cyclohexane:ethyl acetate, 20:1) to yield **3** as a white solid (6.25 g, 78%): mp 58 °C. ^{1}H NMR (250 MHz, $CDCl_3$): δ = 0.89 (t, J = 6.5 Hz, 3H, CH_3), 1.25 (m, 28H, 9-H-23-H), 1.60 (q, J = 7.0 Hz, 2H, 8-H), 2.65 (t, J = 8.0 Hz, 2H, Ar−CH_2), 7.25−7.28 (m, 2H, 3-H, 5-H), 7.53−7.57 (m, 2H, 2-H, 6-H).

4-Heptadecyl-benzamidiniumchloride, 4. A 2 M solution of trimethylaluminum in toluene (7.33 mL, 14.6 mmol) was added slowly at 50 °C under an argon atmosphere to a vigorously stirred suspension of ammonium chloride (0.815 g, 15.2 mmol) in 15 mL of dry toluene (distilled from Na). After addition, the mixture was allowed to warm to room temperature and stirred for 2 h until the gas evolution (methane) has ceased. A solution of 4-heptadecylbenzonitrile (3.0 g, 8.8 mmol) in 10 mL of dry toluene was added, and the mixture was kept 18 h at 80 °C for 18 h. After cooling, the reaction mixture was slowly poured into a slurry of 8 g of silica gel in 50 mL of chloroform and stirred for 10 min. The silica was filtered off and washed several times with methanol. The filtrate and wash were combined, and the solvent was evaporated. The solid residue was extracted with hot acetone and water, leaving the pure product as a colorless solid (2.24 g, 65%): mp 138 °C. ^{1}H NMR (250 MHz, DMSO-[d_6]): δ = 0.83 (t, 3H, CH_3), 1.1−1.4 (m, 30H, $(CH_2)15$), 2.61−2.68 (t, 2H, J = 7.9 Hz, Ar−C$\underline{H}_2$), 7.41 (d, J = 9 Hz, 2H, 3-H, 5-H), 7.83 (d, J = 9 Hz, 2H, 2-H, 6-H), 9.20 (s, 2H, amidinium (*syn*)), 9.34 (s, 2H, amidinium (*anti*)). MS (EI, 70 eV): *m*/*z* (%) = 359(100) [M^+], 160(9), 154(20), 147(40), 134(31), 107 (10).

***p*-Methylbenzamidine, 5.** *p*-Methylbenzonitrile (5.0 g, 42.6 mmol) was dissolved in 50 mL of dry toluene (distilled from Na), treated with a suspension of sodium amide in toluene (50%, 17 mL, 213 mmol), and refluxed for 18 h under argon atmosphere. After cooling to room temperature the reaction mixture was quenched carefully with 5 mL of water and evaporated to dryness. The solid residue was recrystallized from small amounts of acetone to provide a pale yellow solid (1.85 g, 32%): mp 68 °C. ^{1}H NMR (250 MHz, $CDCl_3$): δ = 2.31 (s, 3H, CH_3), 5.62 (s (br), 3H, amidinium), 7.12 (d, J = 9 Hz, 2H, 3-H, 5-H), 7.43 (d, J = 9 Hz, 2H, 2-H, 6-H).

***p*-Methyl-benzamidinium-tetrafluoroborate, 6.** A solution of *p*-methylbenzamidine (1.0 g, 7.45 mmol) in 10 mL of diethyl ether was treated with tetrafluoroboric acid (54%, 1.02 mL, 7.45 mmol) and sonicated for 10 min. The precipitate was filtered off and suspended

(13) Echaverren, A.; Galan, A.; Lehn, J.-M.; de Mendoza, J. *J. Am. Chem. Soc.* **1989**, *111*, 4994.
(14) Mueller, G.; Riede, J.; Schmidtchen, F. P. *Angew. Chem., Int. Ed. Engl.* **1988**, *27*, 1516.
(15) Terfort, A.; von Kiedrowski, G. *Angew. Chem., Int. Ed. Engl.* **1992**, *31*, 654.
(16) Hoffmann, S. *Angew. Chem., Int. Ed. Engl.* **1992**, *31*, 1013.

in 20 mL of acetone, sonicated, and filtered again (1.63 g, 98%). ^{1}H NMR (250 MHz, DMSO-[d_6]): δ = 2.39 (s, 3H, CH_3), 7.43 (d, J = 9 Hz, 2H, 3-H, 5-H), 7.0 (d, J = 9 Hz, 2H, 2-H, 6-H), 8.76 (s, 2H, amidinium (*syn*)), 9.20 (s, 2H, amidinium (*anti*)).

***n*-Tetradecyltriphenylphosphoniumbromide, 7.** 1-Bromotetradecane (34.5 g, 125 mmol) was added to a solution of triphenylphosphane (32.6 g, 125 mmol) in 200 mL of dry acetonitrile. The mixture was refluxed overnight, the solvent removed in vacuo, and the resulting yellow oil treated several times with dry diethyl ether, yielding a white precipitate (53.1 g, 78%) that was used without further purification.

4-(Pentadec-1-enyl)-methylbenzoate, 8. A solution of *n*-tetradecyltriphenylphosphoniumbromide (16.4 g, 30 mmol) in 100 mL of dry THF was treated with *n*-buthyl-lithium (2.5 M in *n*-hexane, 14.4 mL, 36 mmol) resulting in a bright orange solution. The mixture was stirred for 1 h before methyl(4-formyl)benzoate (5.0 g, 30 mmol) dissolved in 20 mL of THF was added drop-by-drop over 1 h. After stirring for 15 h at room temperature the reaction mixture was quenched with 12 mL of acetone, stirred for an additional hour, and filtered over a short column of neutral aluminum oxide to remove all triphenylphosphane-oxide. The solvent was evaporated, and the solid residue was chromatographed on silica gel (cyclohexane:ethyl acetate, 5:1) to yield **8** (5.88 g 52%). ^{1}H NMR (250 MHz, $CDCl_3$): δ = 0.9 (t, 3H, CH3), 1.2−1.5 (m, 26H, $(CH_2)_{13}$), 2.3−2.5 (m, 2H, Ar−CH═CH−CH_2), 3.91 (s, 3H, CH_3), 5.78 (dt, J = 11 Hz, J = 7.5 Hz, 1H, Ar−CH═C$\underline{H}$), 6.36−6.51 (m, 1H, Ar−CH═CH), 7.25−7.44 (m, 2H, 3-H, 5-H), 7.9−8.1 (m, 2H, 2-H, 6-H).

4-Pentadecylmethylbenzoate, 9. 4-(Tetradec-1-enyl)methylbenzoate (3.5 g, 10.1 mmol) was hydrogenated under normal H_2-pressure overnight in 100 mL of a solvent mixture (ethyl acetate:methanol, 1:1) containing 200 mg of Pd/C (10%) as the hydrogenation catalyst. The catalyst was removed by filtration over Celite, and the solvent was evaporated. The crude product was purified by chromatography on silica gel (cyclohexane:ethyl acetate, 40:1) to yield **9** as a white solid (3.3 g, 95%): mp 94 °C. ^{1}H NMR (250 MHz, $CDCl_3$): δ = 0.9 (t, 3H, CH_3), 1.2−1.5 (m, 26H, $(CH_2)_{13}$), 1.6−1.78 (m, 2H, CH_2) 2.7 (t, 2H, Ar−C$\underline{H}_2$), 3.91 (s, 3H, CH_3), 7.25 (d, J = 8 Hz, 2H, 3-H, 5-H), 7.95 (d, J = 8 Hz, 2H, 2-H, 6-H).

4-Pentadecylbenzoic Acid, 10. 4-Pentadecylmethylbenzoate (3.0 g, 8.6 mmol) was dissolved in 50 mL of a 5 N solution of KOH in water/methanol, 1:10 (v/v), and stirred at room temperature for 2 h. The reaction mixture was acidified with HCl, and the white precipitate was filtered off, washed with water, and recrystallized from ethanol to give **10** (1.78 g, 5.3 mmol, 62%) as a white solid: mp 92 °C. ^{1}H NMR (250 MHz, $CDCl_3$): δ = 0.8 (t, 3H, CH_3), 1.1−1.4 (m, 26H, $(CH_2)_{13}$), 1.51−1.62 (m, 2H, CH_2) 2.7 (t, 2H, Ar−CH_2), 7.2 (d, J = 8 Hz, 2H, 3-H, 5-H), 7.85 (d, J = 8 Hz, 2H, 2-H, 6-H).

2.2. Grazing Incidence X-ray Diffraction (GIXD). The GIXD experiments on the Langmuir films were performed on the liquid-surface diffractometer at the synchrotron undulator beamline BW1, HASYLAB (Hamburg Synchrotron laboratory), DESY. The dimensions of the footprint of the incoming X-ray beam on the liquid surface were approximately 5 × 50 mm^2. The synchrotron white beam was monochromated with a beryllium (002) crystal to the wavelength of 1.304 Å, and the incident angle α was adjusted to $0.85\alpha_c$, where $\alpha_c \approx 0.14°$. The scattered intensity was collected by means of a vertical position-sensitive detector, PSD (OED-100-M, Braun, Garching, Germany), which intercepts photons over the range $0 \le q_z \le 0.9$ Å^{-1} (q_z is the vertical component of the X-ray scattering vector). The measurements were performed by scanning across the horizontal component of the scattering vector, q_{xy}, and simultaneously resolving q_z with the PSD. The diffraction data are represented in three ways: as contour plots $I(q_{xy},q_z)$; as a pattern that shows the Bragg peak intensity profiles $I(q_{xy})$ obtained by integrating the whole q_z intensity for any q_{xy} along the measured range, and finally as Bragg rod profiles that show the scattered intensity $I(q_z)$ in channels along the PSD, integrated over the whole range in q_{xy} for a Bragg peak.

The q_{xy} positions of the Bragg peaks yield the lattice repeat distance $d = 2\pi/q_{xy}$, which may be indexed by the two Miller indices h,k to yield the unit cell. The full width at half-maximum (fwhm) in q_{xy} units of a Bragg peak yields the 2D crystalline coherence length associated with the h,k reflection. The fwhm of the Bragg rod profile = Δq_z gives a measure of the thickness of the crystalline film, $T = 0.9(2\pi)/\Delta q_z$. More detailed descriptions of the GIXD method used for monolayer structure determination are given elsewhere.[17,18]

Diluted chloroform solutions of the amphiphilic compounds were spread on Millipore water or on aqueous solutions containing the water-soluble components at ∼15 °C and then cooled to the temperature of 5 °C, at which the GIXD and X-ray reflectivity measurements were performed.

2.3. Single-Crystal X-ray Diffraction Studies. Pentadecylbenzoate and *p*-Methylbenzylamidinium. *p*-Methylbenzamidine and pentadecylbenzoic acid in a 1:1 ratio were mixed in ethyl acetate, and the resulting salt was filtered and redissolved in analytical ethanol. Slow cooling of saturated solutions yielded flat crystalline needles. A suitable single crystal was mounted on an AFC5 Rigaku diffractometer equipped with the rotating anode tube, and the intensity data were measured with the specimen crystal at ambient temperature (17 °C). The crystal structure was solved by direct methods and refined with use of SHELX-97 software.[19] The experimental X-ray data are summarized in Table 4.

***p*-Methylbenzamidinium Benzoate**. Needlelike colorless crystals were grown from water solution by slow evaporation. Structural data and experimental details of single-crystal X-ray diffraction measurements are summarized in Table 4.

3. Results

3.1. Surface Pressure−Molecular Area (π−A) Isotherms. The π−A isotherms of several amphiphilic systems incorporating carboxylic acid and amidinium functions were measured at the air−water (or air−aqueous solution) interface. The surfactants employed were *p*-pentadecylbenzoic acid, $C_{15}H_{31}-C_6H_4-CO_2H$ (labeled C_{15}-benzoic acid), and *p*-heptadecylbenzamidinium $C_{17}H_{35}-C_6H_4-CN_2H_4Cl$ (labeled C_{17}-benzamidinium). Benzamidinium and *p*-methylbenzamidinium ($X-C_6H_4-CN_2H_3$, X = H, CH_3 respectively), sodium benzoate, $C_6H_5-CO_2Na$ were the water-soluble components.

The π−A isotherms of C_{15}-benzoic acid, spread on Millipore water at 5 °C and at 20 °C, indicate a limiting area per molecule of 5−7 Å^2 which is about 5 times smaller than that usually occupied by amphiphilic molecules each bearing a single hydrocarbon chain (Figure 1a, solid line). This observation suggested formation of a multilayer film. Addition of 1.8 mM of KOH into the water subphase yields a limiting area per molecule of 21−22 Å^2 (Figure 1a, long-dashed line) that clearly corresponds to the formation of a monolayer of potassium C_{15}-benzoate.

According to π−*A* isotherm measurements, C_{17}-benzamidinium forms a monolayer on the water surface, (Figure 1b, solid line), with a limiting area per molecule of 23−24 Å^2.

When C_{15}-benzoic acid is spread on a solution containing water-soluble $C_6H_4-CN_2H_3$ or $CH_3-C_6H_4-CN_2H_3$, the isotherm curve becomes expanded with a large kink at $A \approx 30$ Å^2 preceding the plateau region, followed by a second increase of the surface pressure at ∼10 Å^2 (Figure 1a, short-dashed line). The amphiphile C_{17}-benzamidiniumchloride spread on an aqueous subphase containing $C_6H_5-CO_2Na$ yields a similar isotherm (Figure 1b, dashed line). Their shapes resemble the π−A isotherm of the long-chain mandelic acid on phenylethylamine solution.[1]

The influence of the concentration of $C_6H_5-CO_2K$, present within the aqueous subphase, on the degree of expansion of the π−*A* isotherm of C_{17}-benzamidinium was studied before the plateau region (40 Å^2 < *A* < 100 Å^2). There was no

(17) Als-Nielsen, J.; Jacquemain, D.; Kjaer, K.; Leveiller, F.; Lahav, M.; Leiserowitz, L. *Phys. Rep.* **1994**, *246*, 251.
(18) Majewski, J. *Chem. Eur. J.* **1995**, *1*, 304.
(19) Sheldrick, G. M. *Acta Crystallogr.* **1990**, *A46*, 467.

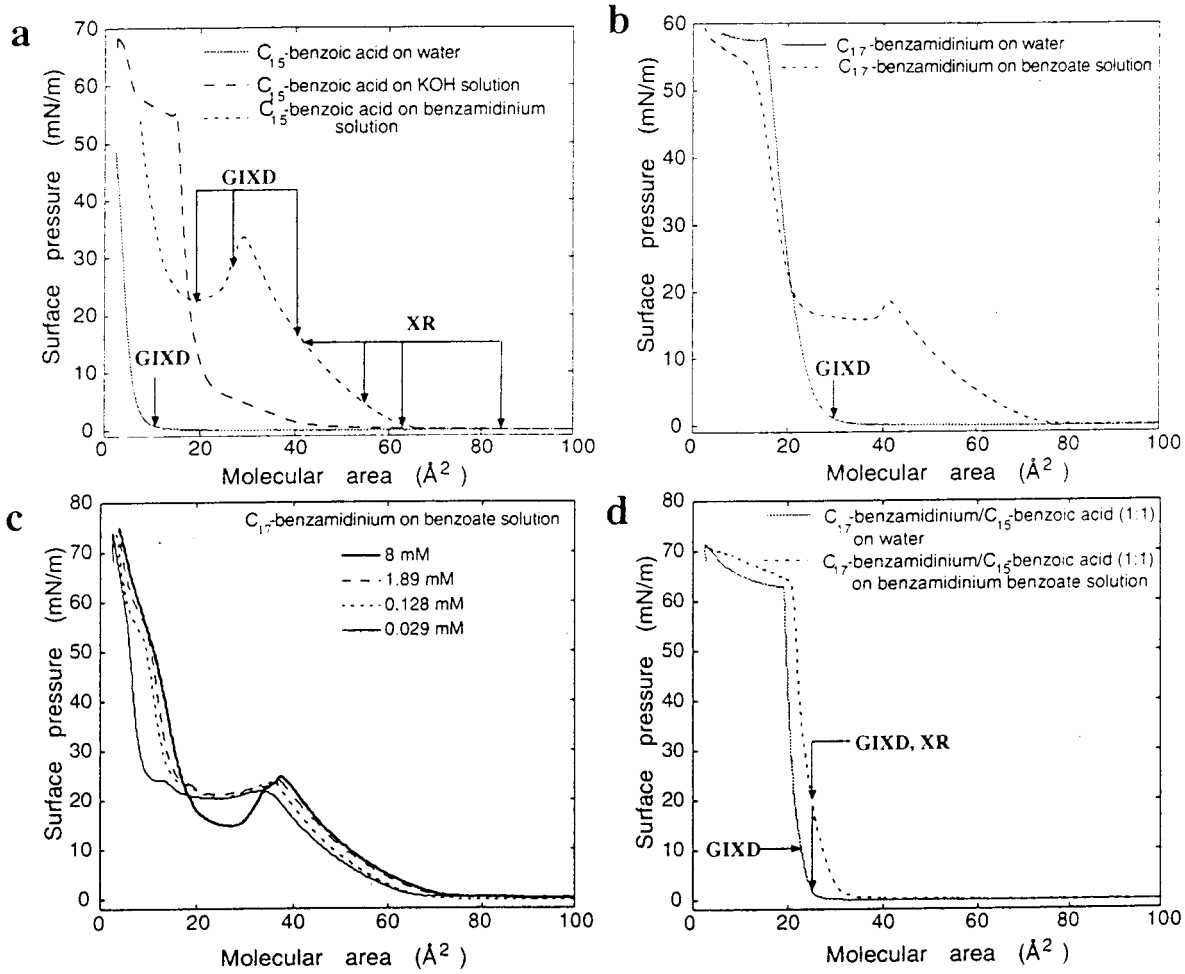

Figure 1. Surface pressure−molecular area isotherms of various systems involving interactions between benzamidinium and benzoate moieties, as described in the inset of each graph and in the text. GIXD and XR measurements were performed in the points marked by arrows.

observable change in the isotherm over a broad range in concentration (3×10^{-5} to 8×10^{-3} M), suggesting that the water-soluble and water-insoluble components always form a 1:1 salt at the air−solution interface (Figure 1c).

The 1:1 mixture of C_{15}-benzoic acid and C_{17}-benzamidinium spread on Millipore water forms a stable monolayer, according to the $\pi-A$ isotherm measurements, with a limiting area per molecule of 24 Å^2 (Figure 1d, solid line). On aqueous solutions of benzamidinium (or methylbenzamidinium) benzoate, the isotherm is generally more expanded. the degree of which depends on the concentration of the water-soluble components (Figure 1d, dashed line).

3.2. Grazing incidence X-ray diffraction (GIXD) measurements. C_{15}-benzoic Acid on Pure Water. The measured GIXD pattern of the acid spread on pure water for a calculated area per molecule of 25 Å^2 contains three reflections with strongly modulated Bragg rods, corresponding to a multilayer with in-plane cell dimensions $a = 6.3$ Å, $b = 5.6$ Å, $\gamma = 100°$, $A_{xy} = 34.7$ Å^2 (Figure 2a). The thickness of the film T is ∼90 Å, as estimated from the average full width at half-maxima (fwhm), $\Delta q_z = 0.06$ Å^{-1}, of the Bragg rod modulations ($T = 0.9(2\pi/\Delta q_z)$). The average Δq_z difference between the neighboring maxima of the Bragg rod modulations corresponds to a spacing of 30.5 Å. On the assumption that the acid molecules form centrosymmetric hydrogen-bonded cyclic dimers, the spacing of 30.5 Å is that of a bilayer. The total number of bilayers, which constitute the film of thickness 90 Å, is therefore equal to three. About the same total number of bilayers is suggested by the ratio between the extrapolated area per molecule from the $\pi-A$ isotherm (5 Å^2) and the unit cell area $A_{xy} = 35$ Å^2. Given the bilayer thickness T of 30.5 Å and an estimate of the length of the C_{15}-benzoic acid molecule, $L_m \approx 52$ Å, we derive the tilt angle t of the chain from the layer normal [t = arc cos-(T/L_m)] to be ∼54°. This value corresponds to a cross-sectional hydrocarbon chain area A_{xy}·cos t of 20 Å^2.

The packing motif of the C_{15}-benzoic acid at the air−water interface is not similar to the 3D packing motif of analogous *p*-heptylbenzoic acid $C_7H_{15}-C_6H_4-CO_2H$, in which the chains are interdigitated.[20] Furthermore, the multilayer formation of C_{15}-benzoic acid at the air−water interface is in contrast to the monolayer assembly of the similar compound 4-(octadecycloxy)-benzoic acid ($C_{16}H_{33}-O-C_6H_4-CO_2H$)[21] and the regular fatty acids.[22−25] A spontaneous multilayer crystalline formation at the air−water interface has been observed previously for α−ω alkane diols,[26] diacids,[27] simple alkanes,[28] and short-chain α-amino acids.[29]

(20) Blake, A. J.; Fallis, I. A.; Parsons, S.; Schroder, M.; Bruce, D. W. *Acta Crystallogr., Sect. C* **1995**, *51*, 2666.
(21) Weissbuch, I.; Berkovic, G.; Yam, R.; Als-Nielsen, J.; Kjaer, K.; Lahav, M.; Leiserowitz, L. *J. Phys. Chem.* **1995**, *99*, 6036.
(22) Peterson, I. R. *Ber. Bunsen-Ges. Phys. Chem.* **1991**, *95*, 1417.
(23) Riviere, S.; Henon, S.; Meunier, J.; Schwartz, D. K.; Tsao, M. W.; Knobler, C. M. *J. Chem. Phys.* **1994**, *101*, 10045.
(24) Peterson, I. R.; Kenn, R. M. *Langmuir* **1994**, *10*, 4645.
(25) Kuzmenko, I.; Kaganer, V. M.; Leiserowitz, L. *Langmuir* **1998**, *14*, 3882.
(26) Popovitz-Biro, R.; Majewski, J.; Margulis, L.; Cohen, S.; Leiserowitz, L.; Lahav, M. *Adv. Mater.* **1994**, *6*, 956.
(27) Weissbuch, I.; Guo, S.; Cohen, S.; Edgar, R.; Howes, P.; Kjaer, K.; Als-Nielsen, J.; Lahav, M.; Leiserowitz, L. *Adv. Mater.* **1998**, *10*, 117.

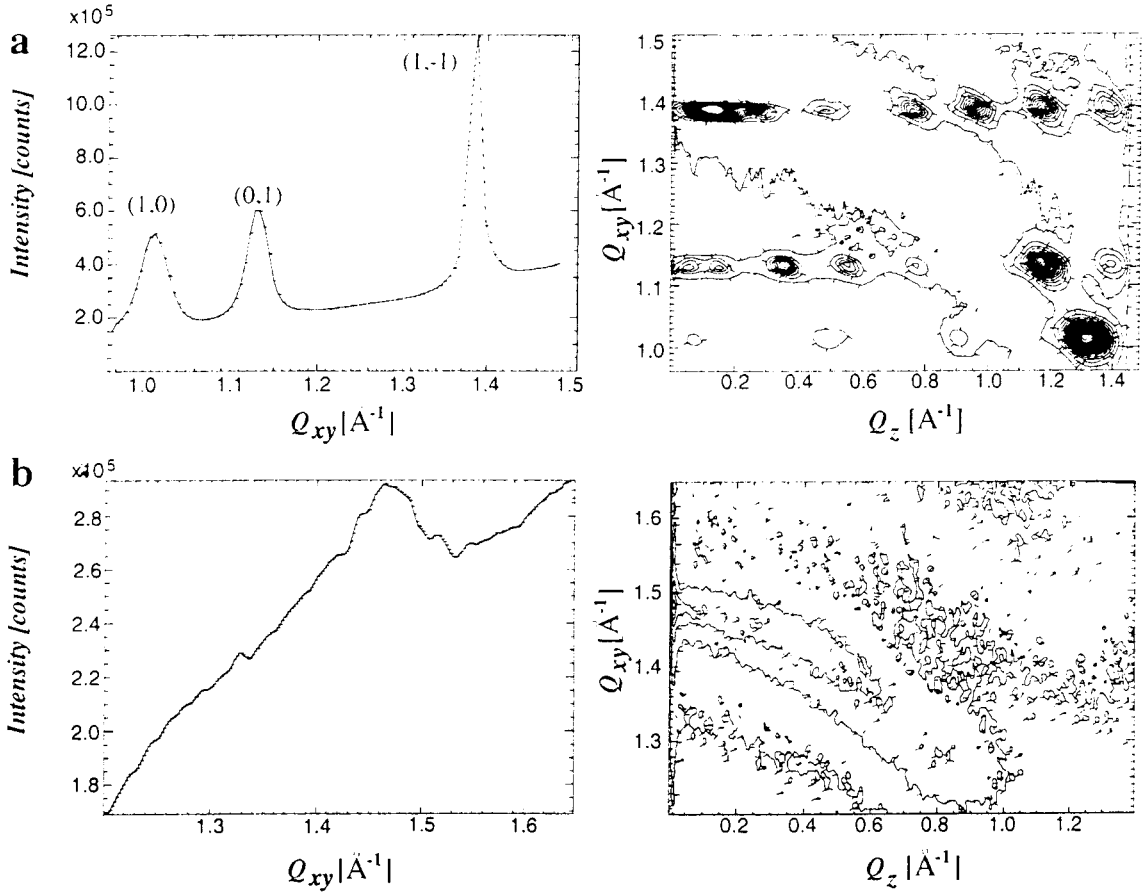

Figure 2. GIXD patterns of (a) C_{15}-benzoic acid, (b) C_{17}-benzamidinium, both on pure Millipore water.

C_{17}-benzamidinium Chloride on Pure Water. The amphiphile was spread on Millipore water for an area per molecule A of 35 Å^2, and the film was compressed until $A = 25$ Å^2, at which point the surface pressure had risen to $\pi = 1$ mN/m. The GIXD pattern contains a very broad peak (Figure 2b), reflecting a high degree of molecular disorder. We attribute the lack of crystalline order as arising from repulsive interactions between positively charged headgroups.

Pentadecylbenzoic Acid on *p*-Methylbenzylamidinium Solution. The amphiphile C_{15}-benzoic acid was spread on aqueous solution containing *p*-methylbenzamidinium (0.008 M) prepared by neutralizing *p*-methylbenzamidinium chloride with an equimolar amount of potassium hydroxide. The GIXD patterns were measured at three points along the $\pi-A$ isotherm: one before the kink at the beginning of the plateau region and the two others along the plateau, as marked by arrows in Figure 1a. In the region before the kink, no Bragg peaks were observed, indicating an amorphous monolayer. The compression to the plateau region gave rise to a diffraction signal. The GIXD pattern measured at $A = 30$ and 20 Å^2 contains seven reflections (Figure 3), five of which are relatively intense, and indexed with an oblique unit cell $a = 10.06$ Å, $b = 5.50$ Å, $\gamma = 83.2°$, $A_{xy} = 54.9$ Å^2. The two remaining peaks (at $q_{xy} = 1.19$ and 1.44 Å^{-1}) of near threshold intensity belong to another crystalline phase, because all seven peaks could be expressed in terms of one unit lattice. This minor crystalline phase will not be further discussed. The unit cell dimensions of the major phase almost match the intralayer cell dimensions of the 3D crystal structure of the same molecular composition ($a = 9.58$ Å, $b = 5.73$ Å, $\gamma = 90°$, $A_{xy} = 54.9$ Å^2, vide infra), and therefore should have a similar packing motif. The interlayer distance d in the film = 26.4 Å as calculated from the average Δq_z difference of the Bragg rod modulations. The unit cell volume in the film (dab sin γ) = 1449 Å^3, is about equal to the corresponding volume of the 3D crystal structure, (abc)/2 = 1438 Å^3. The full thickness of the film $T \approx 80$ Å, as extracted from the fwhm of the Bragg rods, is compatible with 6+ crystalline layers, where the plus sign denotes a partially crystalline top layer incorporating disordered hydrocarbon chains as depicted in Figure 4a. This thickness is just over 3 times that observed for *R*-pentadecylmandelic acid on *R*-phenylethylamine,[1] that contains one interdigitated bilayer and a top layer with disordered chains.

1:1 Monolayer Mixture of Heptadecylbenzamidinium and Pentadecylbenzoic Acid on Pure Water and on Solution Containing *p*-Methylbenzamidinium Benzoate. A 1:1 mixture of the two amphiphiles was spread on Millipore water and on a saturated solution of *p*-methylbenzamidinium benzoate. The GIXD measurements of the monolayer on pure water were performed at two points along the isotherm, at $A = 24$ Å^2, $\pi = 1$ mN/m, and at $A = 22$ Å^2, $\pi = 10$ mN/m. GIXD scans on the solution were made at 24 Å^2 ($\pi = 20$ mN/m). The diffraction pattern in each case contains two peaks corresponding to a rectangular crystalline lattice of plane symmetry $p1g1$ (Table 1, Figure 5a) in which the hydrocarbon chain axes are tilted from the vertical along the b-axis. On water at $A = 24$ Å^2 the rectangular unit cell dimensions are $a = 4.93$ Å, $b = 9.42$ Å. The molecular chains are tilted from the layer normal by 29°. X-ray structure factor calculations with a refined molecular

(28) Weinbach, S. P.; Weissbuch, I.; Kjaer, K.; Bouwman, W. G.; Nielsen, J. A.; Lahav, M.; Leiserowitz, L. *Adv. Mater.* **1995**, *7*, 857.
(29) Weissbuch, I.; Berfeld, M.; Bouwman, W.; Kjaer, K.; Als-Nielsen, J.; Lahav, M.; Leiserowitz, L. *J. Am. Chem. Soc.* **1997**, *119*, 933.

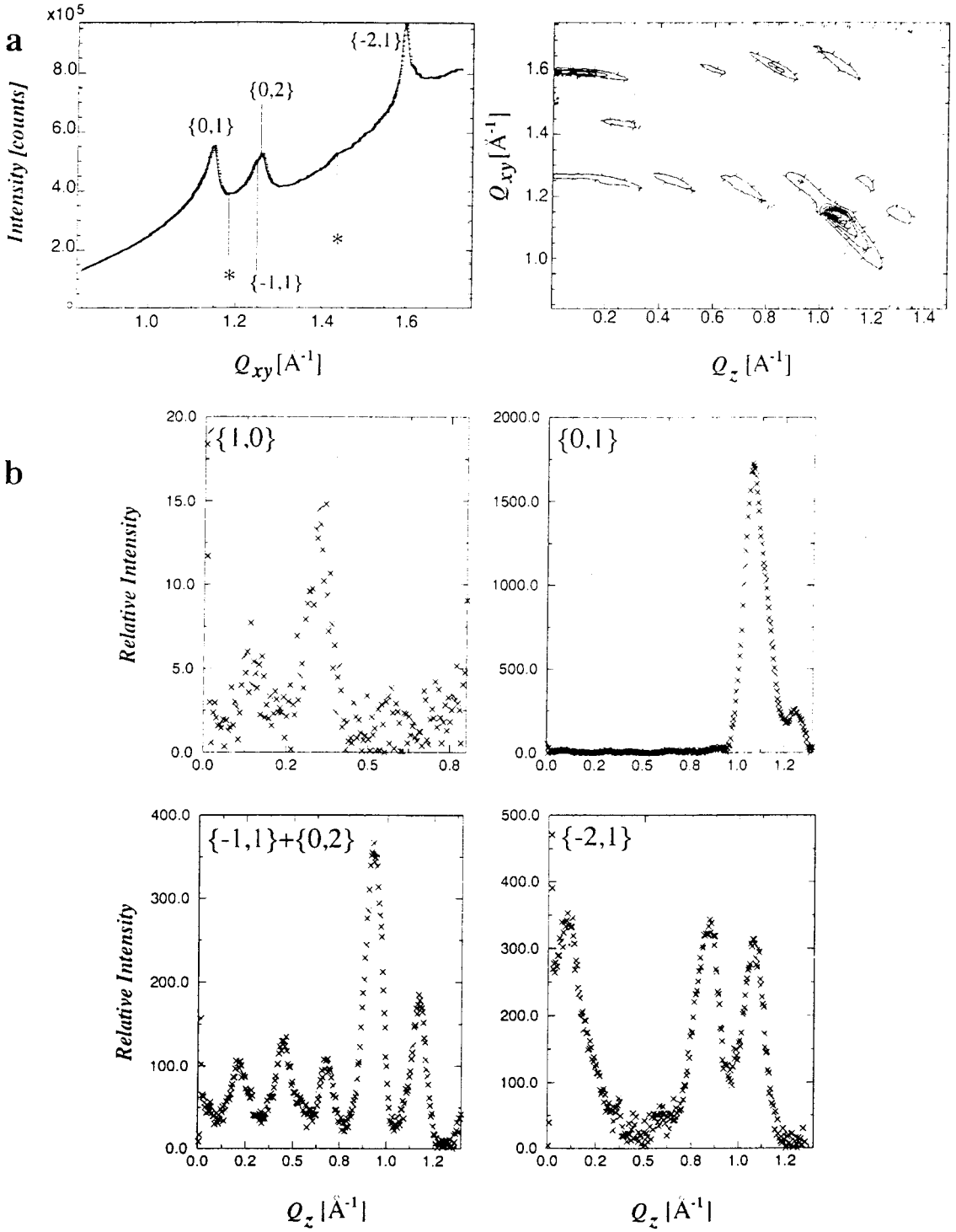

Figure 3. GIXD pattern of C_{15}-benzoic acid spread on *p*-methylbenzamidine (0.008 M), measured at ~20 Å^2

model yielded Bragg rod intensity profiles that fit well to the observed data (Figure 5d,e). On the saturated solution, the molecules are tilted by 24° from the layer normal in a cell of dimensions $a = 4.90$ Å, $b = 9.06$ Å, according to the GIXD pattern (Figure 5c). The decrease in chain tilt from 29° to 24°, reflected in the decrease in length of the *b* axis, can be explained by the increased surface pressure due to the presence of surface-active *p*-methylbenzamidinium benzoate. A GIXD pattern of the monolayer film on pure water studied at a higher surface pressure $\pi = 10$ mN/m (Table 1, Figure 5b) indicates a molecular tilt angle and lattice cell dimensions more akin to those found on the saturated solution.

Here we describe the 1:1 mixed monolayer structure derived from the GIXD data. Three-dimensional crystal structures incorporating amidinium and carboxylic functional groups generally exhibit the linear hydrogen-bonding array shown in Scheme 1b, but with a translation repeat of 9.8 Å twice that of the *a* axis corresponding to the (1,0) spacing of 4.9 Å observed in the mixed monolayer phase. This observation suggests that the hydrogen-bonding array is parallel to the *a*-direction. This array cannot be parallel to the *b*-axis, or even the diagonal $a + b$, since the *b*-axis is reduced in length upon compression (9.4 to 9.0 Å), whereas the *a*-axis remains unchanged but, however, is half of the hydrogen-bonding repeat distance. To overcome

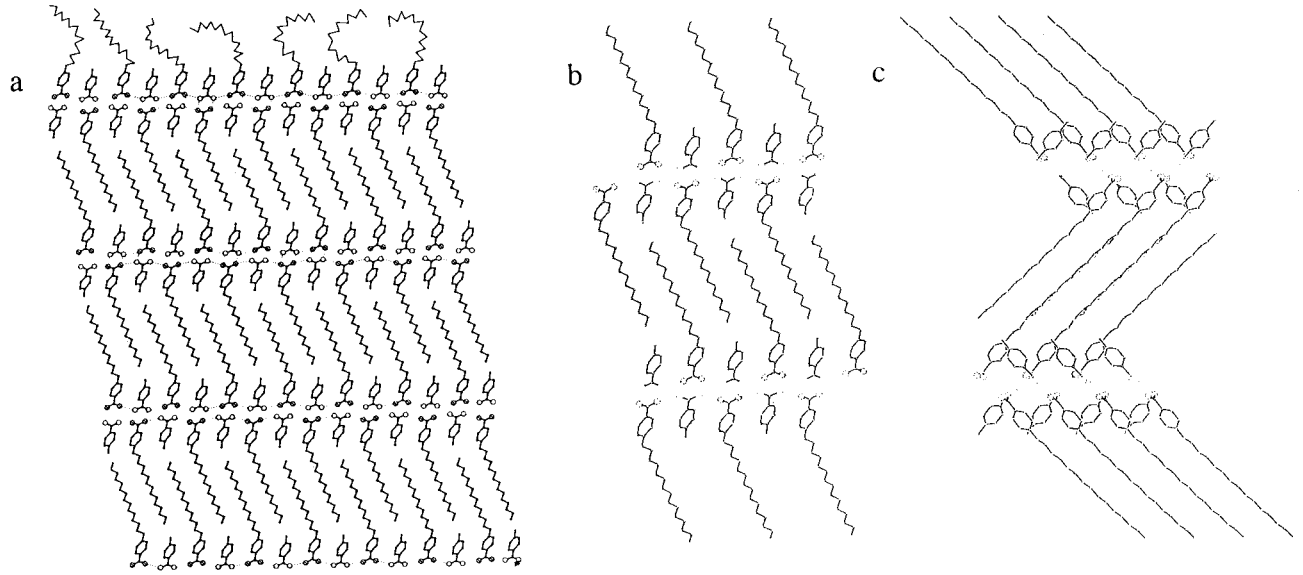

Figure 4. (a) Proposed model packing arrangement of the interdigitated film of *p*-methylbenzamidinium C_{15}-benzoate as formed at the air−solution interface, according to the GIXD data, (b,c) Two views (along *a* and *b*) of the 3D structure of *p*-methylbenzamidinium C_{15}-benzoate.

Table 1. 2D Crystallographic Data[a] from GIXD of the Monolayer of (1:1) C_{17}-benzamidinium and C_{15}-pentadecylbenzoate on Water and on Saturated Solution of *p*-Methylbenzamidinium Benzoate

A_m	π	$I_{(0,2)}/I_{(1,1)}$	a	b	t	A_{xy}	a_o	b_o	A_o
				On Water:					
24	1	0.37	4.93	9.42	29.7	23.2	4.93	8.18	20.1
	10	0.48	4.91	9.11	24.0	22.4	4.91	8.32	20.4
				On Solution:					
24	20	0.48	4.90	9.06	24.1	22.2	4.90	8.27	20.3

[a] π- Surface pressure (in mN/m). A_m- Nominal area per molecule at the water surface. A_{xy} - Unit cell area. A_o - Molecular chain cross-sectional area (Å^2). $I_{(0,2)}/I_{(1,1)}$ - intensity ratio of the (0,2) and (1,1) reflections. *a*,*b*- Unit cell dimensions. a_o,b_o - Unit cell dimensions as projected down the molecular chain axis (Å). Molecular chain tilt - *t* (deg).

this inconsistency, we propose that the hydrogen-bonding arrays with a translation repeat of 9.8 Å are aligned parallel to *a*, but randomly occupying two possible positions along *a* differing by ±9.8/2 Å. (Figure 6). These stacking faults along *b*, smear out the difference between the acid and the amidinium molecules in the diffraction pattern to yield an apparent "repeat" distance along *a* of 4.9 Å. The molecular disorder is also expressed in the relatively low density of the packing of the hydrocarbon chains; the cross-sectional area of the chains are equal to $0.5(ab \cos 29°) = 20.2$ Å^2, compared with 18.7 Å^2 for the standard herringbone chain packing. This result suggests a mesomorphous state of the monolayer.

3.3. Specular X-ray Reflectivity Measurements. Pentadecylbenzoic Acid on Aqueous Subphase Containing *p*-Methylbenzamidinium. The proposed model of the interdigitation process (Scheme 2) implies, as a prerequisite, an amorphous mixed monolayer composed of long-chain amphiphilic acid or base molecules and the corresponding water-soluble counterpart. This model agrees with the isotherm behavior as well as with the GIXD data (no observed diffraction peaks before the plateau region), but direct experimental evidence was provided by specular X-ray reflectivity measurements.

The X-ray reflectivity curves of C_{15}-benzoic acid deposited on aqueous 0.008 M solution of *p*-methylbenzamidinium were measured at four points along the $\pi-A$ isotherm before the plateau region indicated in Figure 1a. The results of these

Table 2. Parameters[a] Fitted to the Observed X-ray Reflectivity Data of *p*-Pentadecylbenzoic Acid on an Aqueous Solution of *p*-Methylbenzamidinium (0.008 M), Assuming a Three-Box Model

A_m	π	N_1	L_1	N_2	L_2	N_3	L_3	σ	t	A_o
85	1	50	1.3	97	1.8	113	5.8	3.5	72	26
64	9	50	1.5	97	2.7	113	7.8	3.4	65	27
55	12	50	2.0	97	2.9	113	8.9	3.5	61	27
44	20[b]	50	2.4	97	4.0	113	10.0	3.8	57	24

[a] A_m - Nominal area per molecule (in Å^2). π - Surface pressure (in mN/m). N_i and L_i ($i = 1,3$) are the number of electrons and box length (in Å). σ - The surface roughness parameter (in Å^2). *t* - Formal value of tilt angle (deg) of the C_{15}-hydrocarbon chain, assuming it is fully stretched and has a length of 18.5 Å, as shown in Figure 7(left). A_o - cross-sectional area (Å^2) occupied by one hydrocarbon chain as calculated based on the molecular tilt *t* and the corresponding A_m. [b] This value corresponds to the maximum value right after the monolayer compression. The pressure was slowly decreasing along the reflectivity measurement due to monolayer relaxation reaching 12 mN/m.

measurements Figure 7(a−d) and the treatment thereof are summarized in Table 2. To fit the experimental curves a fixed molecular area and a three-box model was used with a fixed number of electrons in each box. The model tested incorporates a 1:1 complex of C_{15}-benzoic acid and *p*-methylbenzamidinium. Only the lengths of the three boxes and the surface roughness parameter were refined. The results of the fitting support our interpretation of the expanded region of the $\pi-A$ isotherm. In this region the molecular chains are highly tilted and disordered due to the difference in the cross-sectional area between a hydrocarbon chain (18−20 Å^2) and the sum of the areas occupied by the benzamidinium and benzoic acid headgroups (∼40 Å^2), as shown in Figure 7(top, left). According to the reflectivity analysis, there is a gradual increase in film thickness upon compression, as a result of a corresponding decrease in molecular tilt. We note that there is a clear-cut linear dependence between the thickness L_3 of the disordered hydrocarbon chains and the molecular area *A* (Figure 8). The estimated cross-sectional area per hydrocarbon chain of 24−27 Å^2 is about 15−30% larger than the maximum cross-sectional area observed in mesomorphous monolayer phases incorporating hydrocarbon chains.[25] Such loose packing would account for the lack of a diffraction signal before the plateau region. Once the minimum possible area occupied by the two headgroups is reached (∼40 Å^2), further compression forces the monolayer to buckle and

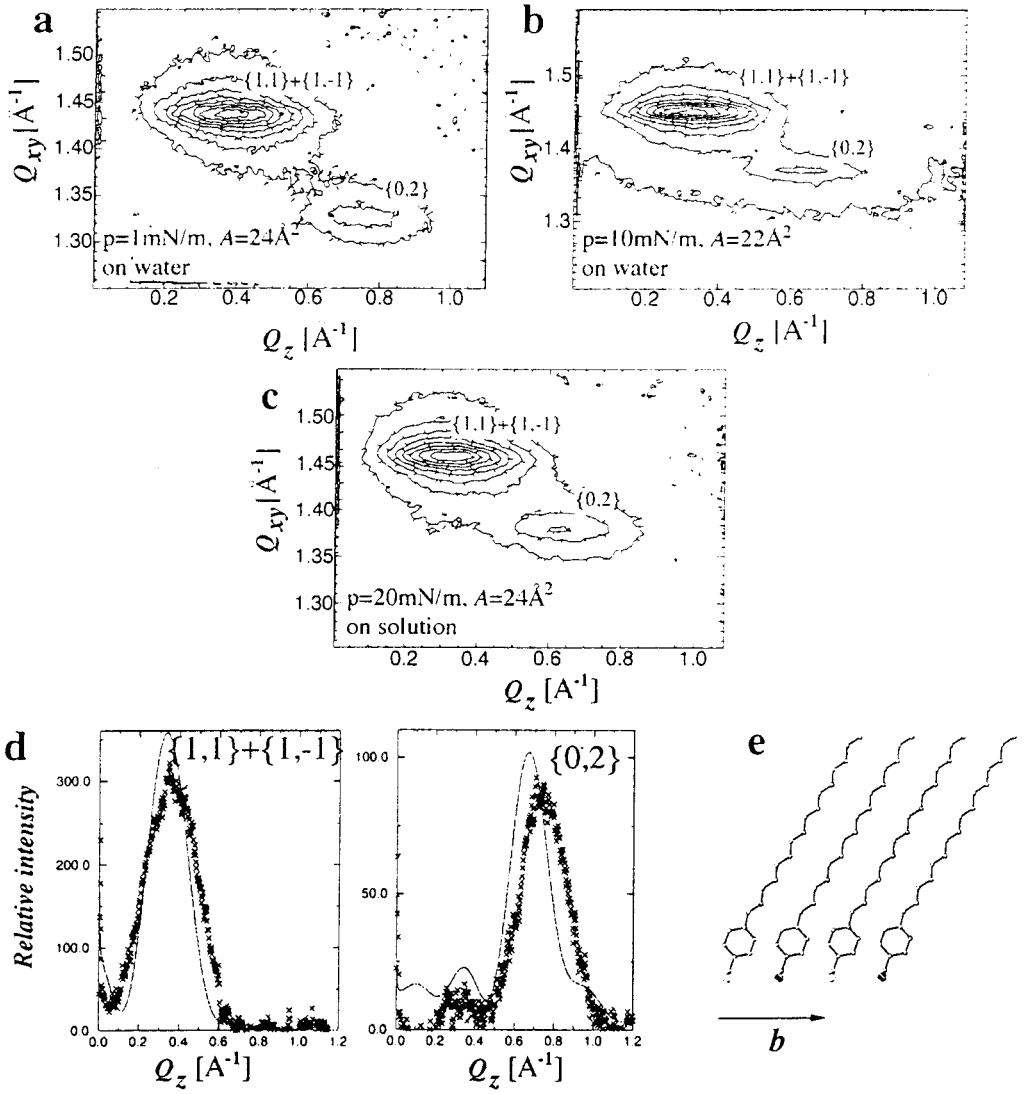

Figure 5. (a−c) GIXD patterns (contour plots) of the mixed monolayer C_{17}-benzamidinium C_{15}-benzoate on water and on solution containing water-soluble benzamidinium benzoate; (d) observed and calculated intensity distribution along the Bragg rods; (e) model packing arrangement corresponding to the calculated curves, presented in (d)

interlayer interdigitation to occur. A detailed description of the buckling process leading to interdigitation is given in the Discussion.

1:1 Mixture of Heptadecylbenzamidinium and Pentadecylbenzoic Acid on Pure Water and on Saturated Aqueous Solution of *p*-Methylbenzamidinium Benzoate. A three-box model was used to calculate a fit to the observed and calculated specular X-ray reflectivity curves from the mixed monolayer on pure water and on the solution subphase containing *p*-methylbenzamidinium benzoate (see Table 3 and Figure 7e,f). The results of this analysis indicate no detectable binding of the solute molecules to the preformed monolayer (Scheme 2).

3.4. Single-Crystal X-ray Diffraction Studies. Pentadecylbenzoate:*p*-Methylbenzamidinium. The 3D crystal structure consists of interdigitated bilayers (Figure 4b,c), as in the 3D crystal structure of *R*-pentadecylmandelate:*R*-phenylethylamine.[1] The present structure displays packing features, characteristic of two reported crystal structures that incorporate only amidinium and carboxylic donor and acceptor functional groups (vide infra). In these two structures the amidinium and carboxylic moieties form heterocyclic hydrogen-bonded dimers (Scheme 1a) interlinked by N−H···O bonds (2.8 Å) to form a continuous array (Scheme 1b) with a translation repeat of 9.6−9.9 Å. This motif is also manifest in the present structure (a = 9.58 Å). The carboxylic and amidinium moieties belonging to the same hydrogen-bonding row form hydrogen-bonding dimers with two neighboring rows along the *b*-axis (Figure 4c), leading to a hydrogen-bonding bilayer network in the *ab* plane. The dihedral angle between the planes of carboxylate and amidinium neighboring species within a row is close to 90°. An analogous motif has been observed in the crystal structure of primary amides defined as the "shallow" glide motif.[30]

Table 3. Parameters[a] Fitted to the Observed X-ray Reflectivity Data of a 1:1 Mixture of Heptadecylbenzamidinium and Pentadecylbenzoic Acid on Pure Water and on a Saturated Aqueous Solution of *p*-Methylbenzamidinium Benzoate

A_m	*cov*	π	N_1	L_1	N_2	L_2	N_3	L_3	σ	t	A_o
On Water											
23	100	1	23	2.3	40	4.1	129	18.0	2.8	31	20
On Solution											
23	95	20	23	3.1	40	4.0	113	19.5	3.0	22	21

[a] The same type of parameters as in Table 2, but for *cov* which is the amphiphilic percentage surface coverage. Molecular tilt t was calculated based on the length of the fully stretched C_{17}-chain = 21 Å and L_3 layer thickness; similar values for t were extracted from the GIXD data (see Table 1).

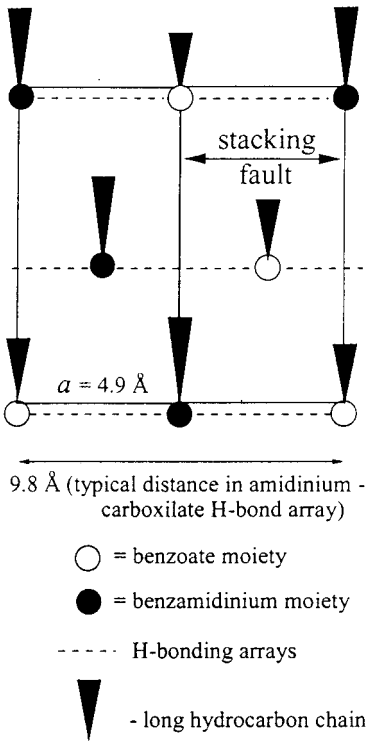

Figure 6. Schematic representation of the molecular disorder in the mixed monolayer C_{17}-benzamidinium C_{15}-benzoate on water and on solution containing water-soluble benzamidinium benzoate

***p*-Methylbenzamidinium:Benzoate.** The analysis of the 3D crystal structure of this compound indicates the N−H···O interactions as given in Scheme 1. However, the amidinium and carboxylic moieties form a channel-like structure rather than the bilayer arrangement, as observed for *p*-methylbenzamidinium:C_{15}-benzoate. The channel incorporates crystallographic 2-fold axis, but a distorted noncrystallographic 4_2 symmetry (Figure 9). Each four-sided channel is constructed from two symmetry-independent cyclic hydrogen-bonded dimers and two more dimers generated by the 2-fold symmetry axis.

4. Discussion

Deposition of *p*-pentadecylbenzoic acid on water containing *p*-methylbenzamidinium yields an amorphous 1:1 acid−base monolayer at the air−water interface. Strong acid−base interactions at the interface result in intercalation of the water-soluble component between the polar headgroups of the amphiphile in the monolayer. According to the X-reflectivity results the monolayer almost doubles in thickness upon reduction in surface molecular area from 85 to 44 Å^2. At the latter area the aromatic rings are aligned almost upright and the hydrocarbon chain occupies a thickness of almost 10 Å^2. This value formally corresponds to highly tilted linear hydrocarbon chains that are poorly packed because of their large surface area of about 40 Å^2 per repeat unit.

Further compression of the film resulted in an overshooting of the isotherm at $A \cong 30$ Å^2 followed by a decrease in surface pressure to a plateau region. Analysis of the GIXD measurements performed along the plateau region of the $\pi-A$ isotherm indicates a transition from the amorphous monolayer to a crystalline multilayer film. The derived unit cell dimensions of the multilayer film are very similar to that of the corresponding macroscopic 3D crystal. The multilayer film comprises three interdigitated bilayers and a top layer that exposes disordered hydrocarbon chains (Figure 4c).

Table 4. Crystallographic Data of the 3D Crystal Structures

	p-methylbenzyl-amidinium: *p*-pentadecylbenzoate	*p*-methylbenz-amidinium benzoate
empirical formula	$C_{30}H_{46}N_2O_2$	$C_{15}H_{16}N_2O_2$
formula weight, g	466.71(3)	256.30(2)
temperature, °C	15	"
wavelength, Å	0.71073	"
crystal system	monoclinic	orthorhombic
space group	$P2_1/n$	*Pba*2
unit cell dimensions:		
a, Å	9.580(2)	18.411(3)
b, Å	5.734(1)	15.954(4)
c, Å	51.99(1)	9.794(2)
β, deg	92.04(2)	90
volume, Å^3	2854.4(3)	2876.8(6)
Z	4	8
density (calc), g/cm^3	1.086	1.184
absorp. coeff., mm^{-1}	0.07	0.08
F(000)	1024.0	1088.0
crystal size, mm^3	0.3 × 0.1 × 0.08	0.3 × 0.3 × 0.6
$2\theta_{max}$ (deg)	60	50
index ranges	$0 < h < 13$, $0 < k < 5$, $-73 < l < 73$	$0 < h < 21$, $0 < k < 18$, $0 < l < 11$
reflections collected	16173	2885
unique reflections	7066	2679
refinement method	full-matrix Least-Squares on F^2	"
weighting scheme	none	"
absorp. correction	none	"
data/parameters	1948/307	1593/336
goodness-of-fit on F^2	1.549	0.894
R ($F_0 > 4\sigma(F_0)$)	0.1019	0.0717
largest ρ (e/Å^3) peak and hole	0.35 and −0.31	0.16 and −0.15

We now address the question how such crystalline multilayers are formed on compression. An economic way to release stress upon compression of Langmuir monolayers may be achieved by a buckling process yielding a corrugated film according to experimental[31−34] and theoretical studies.[35,36] In the Appendix we describe a simple model for the monolayer buckling. The model assumes buckling into a one-dimensional ordered array of inverted arcs, which are connected at line defects (Figure 10). It contains two basic energy parameters: one is the bending constant κ that determines the energy cost for bending the monolayer, the other is the line energy ϵ of the defect, which is *negative* by virtue of the acid−base headgroup attraction. Given these parameters the critical pressure for buckling is predicted to be $\pi^* \cong \sigma_o - {}^3/_4\epsilon^2/\kappa$ where σ_o is the air−water surface tension. The pressure−area isotherm in the buckling region is predicted to be concave down (Figure 12) that is consistent with the shape of the upward part of the measured overshoot (Figure 1a), from which we derive the buckling transition point. This estimate for the transition point appears to give a reasonable value for ϵ. The calculated wavelength of the buckled structure is 50−100 Å. This value is close to the period of about 200 Å

(30) Leiserowitz, L.; Hagler, A. T. *Proc. R. Soc. London* **1983**, *A388*, 133.

(31) Saint-Jalmes, A.; Gallet, F. *Eur. Phys. J. B.* **1998**, *2*, 489; Saint-Jalmes, A.; Graner, F.; Gallet, F. *Europhys. Lett.* **1994**, *28*, 565.

(32) Bourdieu, L.; Daillant, J.; Chatenay, D.; Braslau, A.; Colson, D. *Phys. Rev. Lett.* **1994**, *72*, 1502.

(33) Fontaine, P.; Daillant, J.; Guenoun, P.; Alba, M.; Braslau, A.; Mays, J. W.; Petit, J.-M.; Rieutord, F. *J. Phys. II Fr.* **1997**, *7*, 401.

(34) Lip, M. M.; Lee, K. Y. C.; Takamoto, D. Y.; Zasadzinski, J. A.; Waring, A. J. *Phys. Rev. Lett.* **1998**, *81*, 1650.

(35) Milner, S. T.; Joanny, J.-F.; Pincus, P. *Europhys. Lett.* **1989**, *9*, 495.

(36) Hu, J.-G.; Granek, R. *J. Phys. II Fr.* **1996**, *6*, 999.

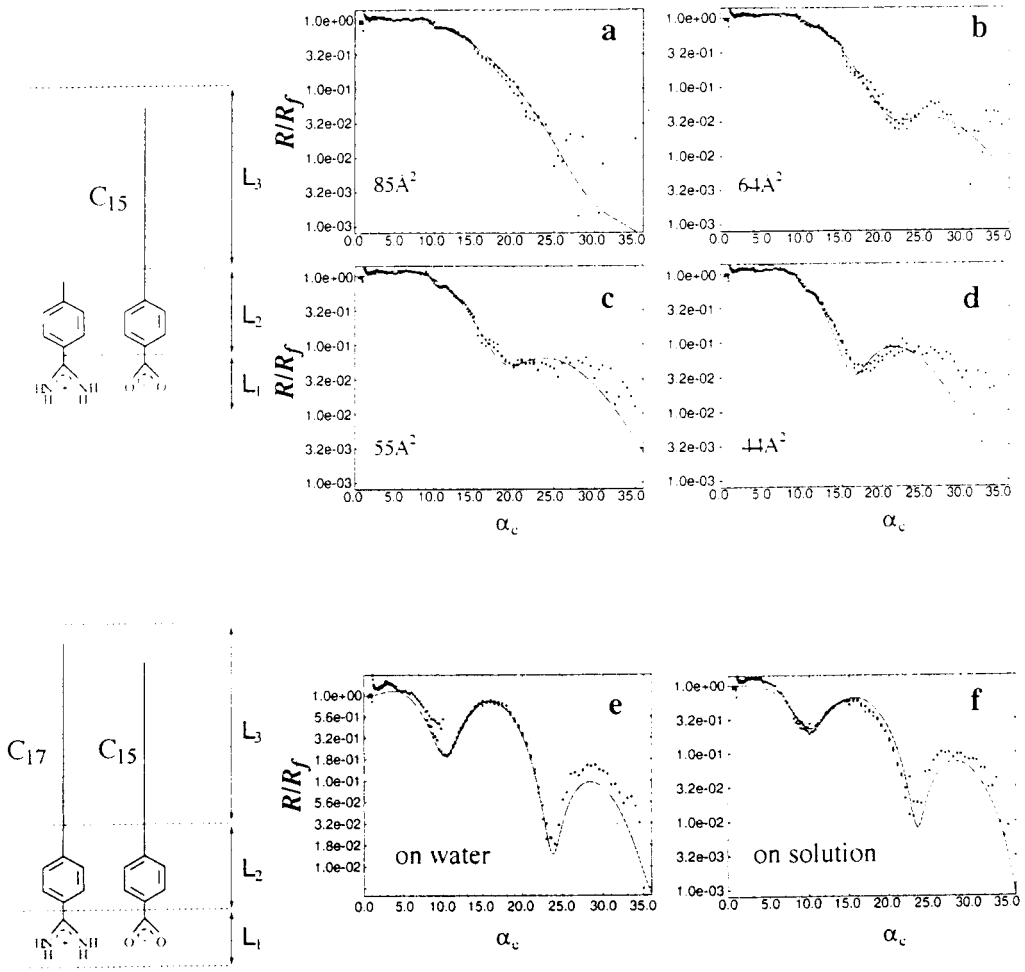

Figure 7. X-ray reflectivity measured and calculated intensity profiles for: (a−d) C_{15}-benzoate on *p*-methylbenzamidinium solution at different compression ratios and for (e,f) C_{17}-benzamidinium C_{15}-benzoate on pure water and on saturated solution of benzamidinium benzoate

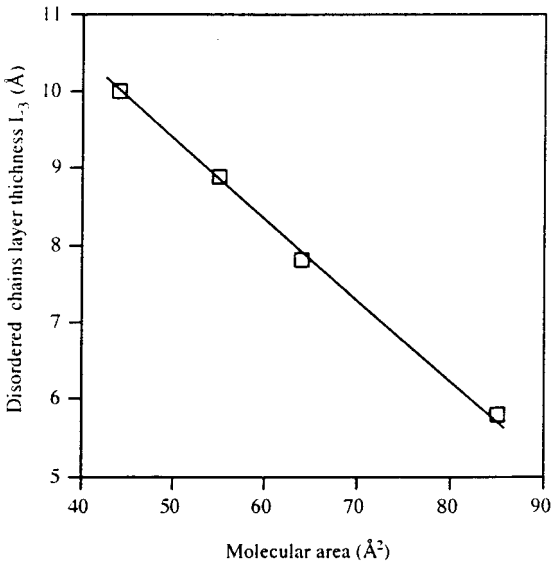

Figure 8. Linear relation between the thickness L_3 of the disordered hydrocarbon chains and the molecular area *A* of the monolayer model structure of C_{15}-benzoic acid and *p*-methylbenzamidinium in a molar 1:1 ratio (see Table 2).

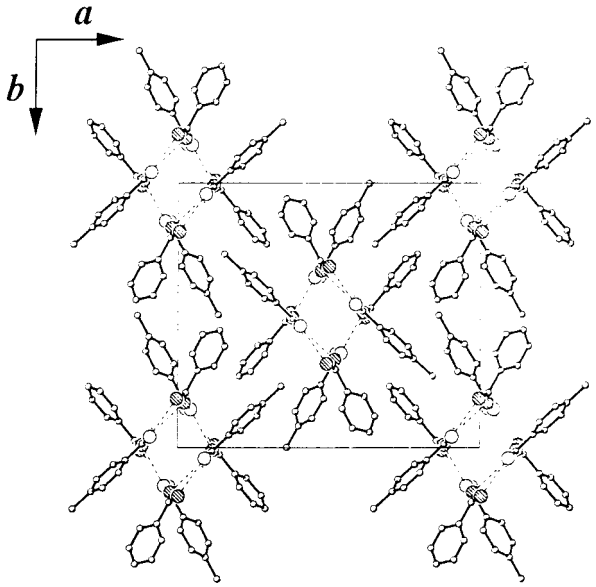

Figure 9. 3D Packing arrangement of *p*-methylbenzamidinium benzoate viewed along the *c*-axis.

established by a GIXD experiment on a monolayer film of arachidic acid on $CdCl_2$ solution at high pH that exhibited a corrugated structure.[37]

In a previous study[1] we had invoked the presence for a buckled monolayer of pentadecyl-mandelic acid and phenylethylamine, leading to a "finger", to explain the formation of the crystalline 2+ layers composed of an interdigitated crystal-

(37) Fradin, C.; Braslau, A.; Luzet, D.; Alba, M.; Gourir, C.; Daillant, J.; Grubel, G.; Vignaud, G.; Legrand, J. F.; Lal, J.; Petit, J. M.; Rietord, F. *Physica B* **1998**, *248*, 310.

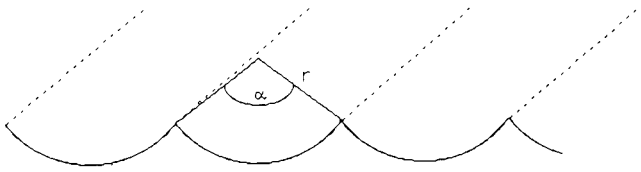

Figure 10. Schematic illustration of the buckled monolayer according to the model described in the Appendix. The line-defects connecting the arcs, denoted by short-dashed lines, are in the direction perpendicular to the plane of the page.

Scheme 3

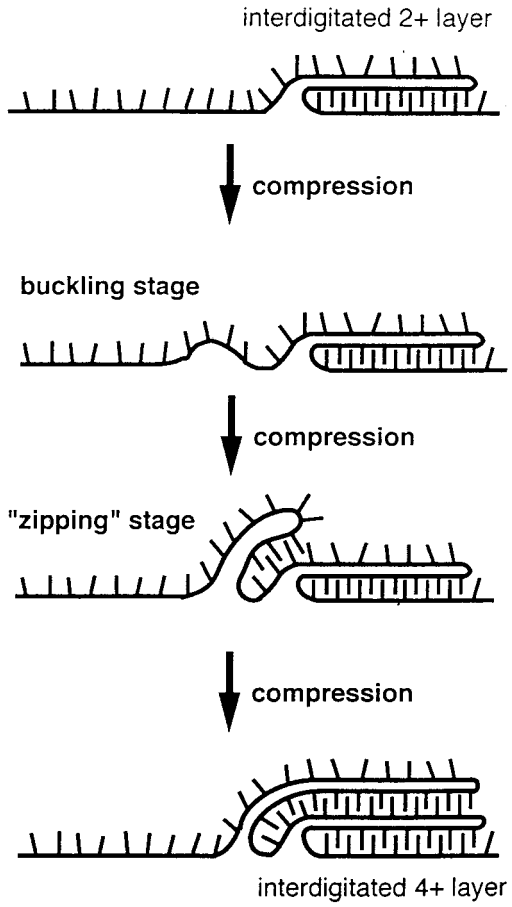

line bilayer and a top layer whose hydrocarbon chains are disordered. For the formation of the 4+ or 6+ layers as found in the compressed film of *p*-pentadecylbenzoic acid and *p*-methylbenzamidinium, a model may be invoked in which individual domains comprise "fingers" of 2+ layers as shown in Scheme 3. Further compression bringing such fingers into proximity can lead to a 4+ layer system as depicted in Scheme 3, and by a similar route to the 6+ layer.

The second goal of the present work was to use the amphiphilic polar headgroups of the crystalline mixed acid−base monolayer as a template for induced complementary binding of the water-soluble acid and amidinium ions at the air−solution interface via hydrogen bonds. However, the X-ray reflectivity studies presented here did not indicate binding of the solute molecules to the monolayer film. It has been established that in aqueous solution there is no observed binding between the carboxylate and amidinium moieties.[7] On the other hand we might have expected binding to occur at the air−solution interface by virtue of cooperative hydrogen bonding as indeed observed in the 3D crystal structure of the analogous interdigitated system. For example, crystalline monolayers of long-chain zwitterionic amino acids induce binding thereto of a layer of glycine or of glutamine molecules by hydrogen bonds, according to epitaxial crystallization and X-ray reflectivity studies. In the present system we tend to account for the absence of binding because the hydrogen-bonding patterns of the monolayer template and that of the 3D crystal structure of the *p*-methylbenzamidinium benzoate are distinctly different, unlike those of the amino acids.

To achieve binding at the air−solution interface appropriate for replication other types of molecular interactions should be considered. Experiments involving binding between an amphiphilic functionalized nucleic acid base pair and its water-soluble complement at the air−water interface has been reported.[40] Therefore, we propose to use a mixture of long-chain nucleic acid base pairs as a template for the binding of the complementary water-soluble base pairs at the air−water interface.

Acknowledgment. We thank the German Israeli Foundation (GIF); Research Grant Marvin Reinstein; the G. M. J. Schmidt Minerva Centre of Supramolecular Architectures, the Danish Foundation for Natural Sciences (DanSync Program), and the European Community (TMR Contract ERBFM-GECT950059) for their support We are grateful to HASYLAB at DESY for X-ray synchrotron beamtime.

Appendix: A Simple Model for Monolayer Buckling

Here we present a simple model that includes the main driving force for buckling in this system. Models for buckling in other monolayer systems are discussed elsewhere.[36] Let us consider a one-dimensional buckling array, which, in its cross section, is simply a collection of inverse arcs (see Figure 10). The buckles are thus connected at singular line defects. We shall assume that the acid−base attraction is the one that controls the line-defect energy, and thus it will be assumed attractive. Even though the microscopic structure of this defect is loosely defined, it is simply viewed as a portion of a bilayer—similar in its microscopic structure to the one in the final (multilayer) state—which is only a single headgroup wide (but macroscopically long).

Let ϵ be the *maximum* strength of the line energy (energy per unit length) of the defect, that is, the energy per unit length when the headgroups are at most close proximity; let σ be the surface tension $\sigma = \sigma_o - \pi$, where σ_o is the water−air surface tension and π the external pressure; let κ be the bending modulus (units of energy).[38] With these parameters, simple dimensional analysis dictates that the critical tension σ^* for buckling into the array described above should scale as $\sigma^* \approx \epsilon^2/\kappa$. This will be confirmed below.

We define r as the radius of curvature of each arc and α as the arc opening-angle (Figure 10). The period of the buckling structure is thus given by $\lambda = 2r \sin(\alpha/2)$, and its amplitude is $U = r - r\cos(\alpha/2)$. We now calculate the Helmholtz free-energy F of the system whose size is L^2 (L is the linear dimension). Consider first the Helfrich bending free-energy.[38] Here we shall neglect the spontaneous curvature C_o since we expect $\kappa C_o^2 \ll \epsilon^2/\kappa$. The bending free-energy of one stripe is thus[38]

(38) Helfrich, W. F. Z. *Naturforsch.* **1973**, *28c*, 693.
(39) Ben-Shaul, A. In *Structure and Dynamics of Membranes*; Lipowsky, R., Sackmann, E., Eds.; Elsevier: Amsterdam, 1995; Chapter 7 and references therein.
(40) Ariga, K.; Kunitake, T. *Acc. Chem. Res.* **1998**, *31*, 371−378.

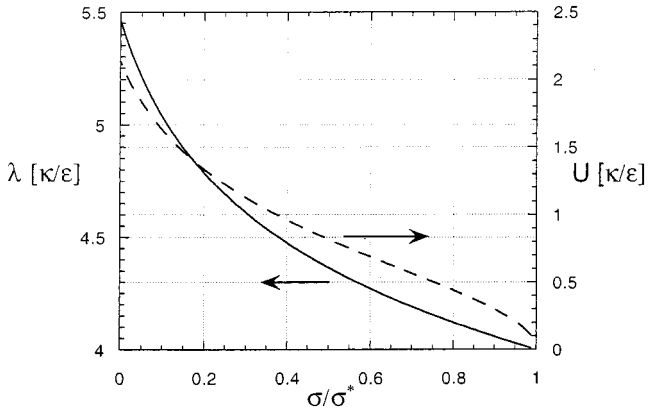

Figure 11. Buckling wavelength λ and buckling amplitude U against the ratio of surface tension $\sigma = \sigma_o - \pi$ to critical tension σ^*, which is a measure of the relative distance from the buckling transition. Both λ and U are measured in units of κ/ϵ, the ratio of bending modulus to line energy.

$$\epsilon_{\text{bend}} = \frac{\kappa}{2r^2}\alpha r L \tag{1}$$

We shall assume that for all angles $\alpha < \pi = 180°$ the deviation of the line energy from its maximum value ϵ (at $\alpha = \pi = 180°$) is determined by the increase in distance between the opposing acid and base headgroups, and this deviation will be calculated within the harmonic approximation. Therefore, the dependence of line energy on α is

$$\epsilon_{\text{line}} = -\epsilon L \sin^2(\alpha/2) \tag{2}$$

The free-energy density $f = F/L^2$ is thus

$$f = \frac{\frac{\alpha}{2}\frac{\kappa}{r} - \epsilon \sin^2(\alpha/2) + \sigma\alpha r}{2r \sin(\alpha/2)} \tag{3}$$

The free-energy eq 1 is now minimized with respect to α and r. The buckling transition is defined as the value of σ (or π) at which α changes from zero to a positive value. Minimizing over r we obtain the relation

$$r = \frac{\kappa}{\epsilon}\frac{\alpha}{\sin^2\alpha} \tag{4}$$

Minimizing over α and using eq 4 we find

$$\frac{\kappa\sigma}{\epsilon^2} \equiv \tilde{\sigma}(\alpha); \quad \tilde{\sigma}(\alpha) = \frac{\sin^3(\alpha/2)(2\sin(\alpha/2) - 3\alpha\cos(\alpha/2))}{2\alpha^2(\alpha\cot(\alpha/2) - 2)} \tag{5}$$

Plotting $\tilde{\sigma}(\alpha)$ against α, we find that it is a monotonically decreasing function starting at a value $\tilde{\sigma}(0) = 3/4$. Thus the critical tension for buckling is

$$\sigma^* = \frac{3}{4}\frac{\epsilon^2}{\kappa} \tag{6}$$

obeying the expected scaling. The buckling transition is a second-order one. To find how α and r, and hence λ and U, change as σ is decreased below σ^*, we need to solve eq 5 numerically. In Figure 11 we plot the resulting λ and U, in units of κ/ϵ, for $0 < \sigma/\sigma^* < 1$. It is seen that λ remains in the range $4 - 5.5 \times \kappa/\epsilon$, whereas U increases from zero to about $2\kappa/\epsilon$.

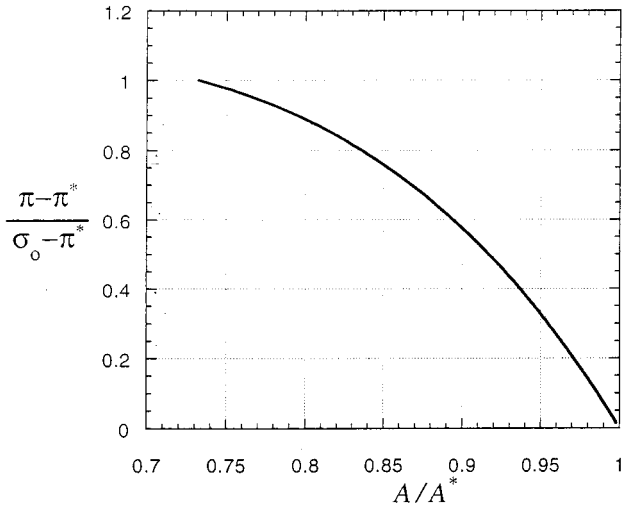

Figure 12. Trough pressure π against trough area A for the buckled monolayer. The pressure is normalized to $(\pi - \pi^*)/(\sigma_o - \pi^*)$, where π^* is the buckling critical pressure and σ_o is the air−water surface tension, as a measure of the relative distance from the buckling transition. The area is normalized to A/A^* where A^* is the critical trough area. The plot does not depend on the model energy parameters.

Using these results, we can calculate the predicted pressure area isotherm, if we assume that the area per molecule on the buckled surface does not change during compression. Even though this cannot be exactly so, it is expected to be a good approximation. Therefore the change in the *projected* area (per molecule), which is the area measured by the Langmuir trough, is purely due to buckling. Using $\sigma = \sigma_o - \pi$, where σ_o is the air−water surface tension, we find the following relation

$$\frac{\pi - \pi^*}{\sigma_o - \pi^*} = 1 - \frac{4}{3}\tilde{\sigma}(\alpha) \tag{7}$$

The ratio of projected area A to the real area, which (as discussed above) is assumed to be equal to the critical area A*, is related to α by

$$\frac{A}{A^*} = \frac{2\sin(\alpha/2)}{\alpha} \tag{8}$$

Using these relations we plot in Figure 12 $(\pi - \pi^*)/(\sigma_o - \pi^*)$ against A/A^*. This plot is universal (within the model assumptions), that is, it is independent of κ and ϵ. Note that the overall shape of the isotherm is *concave down*, although it is, in fact, linear close to criticality, $(\pi - \pi^*)/(\sigma_o - \pi^*) \cong (37/5)(1 - A/A^*)$

Since direct evidence for buckling in this system is yet to be obtained, we have to rely on the experimental $\pi - A$ isotherm. In principle, a singular change in the slope has to be observed at the buckling transition if it is second-order. This, however, may be a too small change to be observed. Nonetheless, the above calculation also shows that the shape of the curve in the buckling region has to be concave down, whereas for a flat monolayer it should always remain convex, for example, as in the case of an ideal gas ($\pi = k_B T/A$). This means that the buckling transition can be assumed to occur if there is an inflection point in the isotherm, that is, when $\partial\pi/\partial A$ reaches a minimum, signifying a transition from convex to concave shape. For the isotherm of the C_{15}-benzoic acid on benzamidinium solution (see Figure 1a), it is possible (even though somewhat difficult) to detect such an inflection point (before the turndown

of the overshoot) at about $\pi' = 27$ dyn/cm, slightly above the monolayer-trilayer coexistence $\pi_c = 23$ dyn/cm.

By using calculations of Ben-Shaul and co-workers,[39] the bending constant due to alkane-tail conformations is roughly $10k_BT/n/10)^{3.2}$ $(a_o/32)^{-7.5}$, where n is the number of CH_2 units and a_o is the area per headgroup measured in $Å^2$. Thus, for a typical area in the range of $a_o = 35 - 40$ A^2 and $n = 15$, we estimate κ in the range $7 - 18k_BT$. Using eq 6 for σ^*, this implies $\epsilon \cong 4 \pm 1 \times 10^{-6}$. Since the linear size of a single headgroup consisting of an acid−base pair is about 10 Å, we find that the *net* attraction between two such headgroups is about $4 \pm 1 \times 10^{-13}$ erg $\cong 10 \pm 2$ k_BT ($\cong 6 \pm 1$ kcal mol^{-1}), which is a reasonable number. It is, however, difficult to get an independent estimate for this energy, since it involves accurate counting of hydrogen bonds formed between acid and base groups in the bilayer configuration and the number of hydrogen bonds broken in dehydration. With these estimates, the basic scale κ/ϵ is estimated to be about 10−20 Å. This implies, for instance, that the wavelength λ is in the range 50−100 Å, which is quite small. It is just sufficiently longer than the size of an headgroup to make our continuum approach valid.

JA002597O